Development of 6-substituted indolylquinolinones as potent Chek1 kinase inhibitors

Shaei Huang,[a,*] Robert M. Garbaccio,[a] Mark E. Fraley,[a] Justin Steen,[a]
Constantine Kreatsoulas,[a] George Hartman,[a] Steve Stirdivant,[b] Bob Drakas,[b]
Keith Rickert,[b] Eileen Walsh,[b] Kelly Hamilton,[b] Carolyn A. Buser,[b] James Hardwick,[b]
Xianzhi Mao,[b] Marc Abrams,[b] Steve Beck,[b] Weikang Tao,[b] Rob Lobell,[b]
Laura Sepp-Lorenzino,[b] Youwei Yan,[c] Mari Ikuta,[c] Joan Zugay Murphy,[c]
Vinod Sardana,[c] Sanjeev Munshi,[c] Lawrence Kuo,[c] Michael Reilly[d] and Elizabeth Mahan[d]

[a]Department of Medicinal Chemistry, Merck Research Laboratories, West Point, PA 19486, USA
[b]Department of Cancer Research, Merck Research Laboratories, West Point, PA 19486, USA
[c]Department of Structural Biology, Merck Research Laboratories, West Point, PA 19486, USA
[d]Department of Drug Metabolism, Merck Research Laboratories, West Point, PA 19486, USA

Abstract—Through a comparison of X-ray co-crystallographic data for **1** and **2** in the Chek1 active site, it was hypothesized that the affinity of the indolylquinolinone series (**2**) for Chek1 kinase would be improved via C6 substitution into the hydrophobic region I (HI) pocket. An efficient route to 6-bromo-3-indolyl-quinolinone (**9**) was developed, and this series was rapidly optimized for potency by modification at C6. A general trend was observed among these low nanomolar Chek1 inhibitors that compounds with multiple basic amines, or elevated polar surface area (PSA) exhibited poor cell potency. Minimization of these parameters (basic amines, PSA) resulted in Chek1 inhibitors with improved cell potency, and preliminary pharmacokinetic data are presented for several of these compounds.
© 2006 Elsevier Ltd. All rights reserved.

Despite their inherent toxicity, DNA damaging agents continue to remain central in clinical cancer chemotherapy. Therefore, strategies directed at improving their therapeutic index are warranted. Following DNA damage, normal cells arrest and attempt repair at the cell cycle checkpoint G1, via the tumor suppressor protein p53, and at G2 and S via the checkpoint kinase Chek1.[1–3] Tumor cells, however often are deficient in the G1 checkpoint due to loss of p53 function (estimated 50–70% of all cancers) and thus, must rely on the checkpoint kinase Chek1 to induce arrest at the S and G2 phases for survival. These p53-deficient cancers should be more vulnerable to Chek1 inhibition which results in abrogation of DNA-damage-induced arrest and premature progression into mitosis resulting in mitotic catastrophe and apoptosis. To summarize, abrogation of the S and G2 checkpoints should sensitize cancer cells to DNA damaging agents in p53-deficient backgrounds without enhancing toxicity toward non-malignant cells. As such, Chek1 inhibitors[4] have the potential to widen the therapeutic window for clinically utilized DNA damaging agents in p53-deficient tumors.

Through comparison of the inhibitor-bound crystal structures (Figs. 1 and 2[5]) of ATP-competitive HTS leads
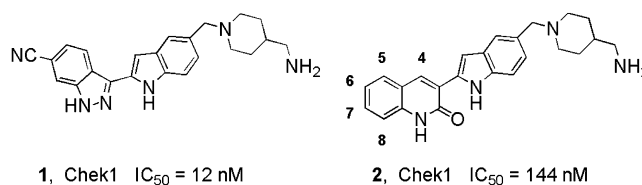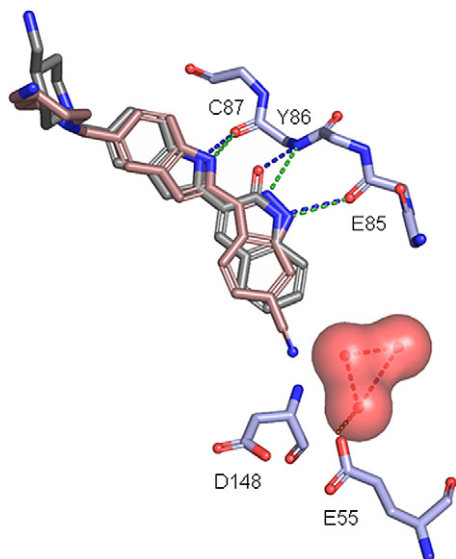
Figure 1. Chek1 inhibitor leads **1** and **2**.

1, Chek1 IC$_{50}$ = 12 nM   2, Chek1 IC$_{50}$ = 144 nM

Figure 2. X-ray crystallographic structures of 1 (salmon) and 2 (gray) bound to Chek1 (light blue) and their hydrogen bonds are shown in dashed green and blue lines, respectively. Three conserved water molecules found in H1 are shown as red spheres with their hydrogen bonding network (dashed red lines).

1[6] and 2 with Chek1, it was hypothesized that placement of substituents at C6 of the indolylquinolinone (2) would best mimic the potency-enhancing C6-CN in 1. This substitution was envisioned to fill a hydrophobic pocket (HI),[7] which is adjacent to the Chek1 ATP-binding site that has been utilized by others.[8,9] In this paper, we report the synthesis, preliminary structure–activity relationship and pharmacokinetic properties of 6-substituted indolyl-quinolinones. Another report has appeared that shows an alternative path for optimization of this series for Chek1 via C4 substitution.[10]

Indolylquinolinone analogs were prepared using the general reaction sequence shown in Scheme 1.[11] 4-Bro-mo-2-iodoaniline reacted regioselectively with methyl acrylate in a microwave promoted Heck-coupling to

afford (E)-methyl 2-amino-5-bromocinnamate 4 in 95% yield. Quinolinone formation was effected by intramolecular cyclization of 4 in ethylene glycol at 200 °C to yield 6-bromo-quinolinone 5.[12] Treatment of 5 with $POCl_3$ gave chloroquinoline 6. Regioselective deprotonation[13] was accomplished by LDA and the resulting anion reacted with 1-chloro-2-iodoethane to provide the 3-iodo-quinoline 7. Hydrolysis of 7 gave 6-bromo-3-iodo-quinolinone 8. Suzuki coupling of 8 with Boc-protected-indolyl boronic acid afforded indolyl-quinolinone 9.[14] Removal of the TBS group, followed by oxidation with Dess-Martin Periodinane yielded aldehyde 10. Reductive amination with various amines in the presence of $NaBH(OAc)_3$ afforded 11. Deprotection of the Boc group, followed by Suzuki coupling with various boronic acids gave indolylquinolinones 13.

Unsubstituted indolylquinolinone 2 has moderate Chek1 inhibitory activity[15] (IC_{50} = 144 nM). Through positional scanning on the quinolinone with a CN group, compound 17 (Table 1) confirmed that C6 was the optimal locus for potency enhancement (>30-fold potency increase over 2). Furthermore, conversion of the nitrile 17 to the amide 18 resulted in an additional 6-fold enhancement of potency. Despite the intrinsic potency of 17 and 18, these Chek1 inhibitors exhibited only weak activity in our cellular checkpoint escape assay[16] (CEA) which measures a compound's ability to release H1299 tumor cells from Camptothecin-induced cell cycle arrest. It was suspected that the presence of two basic amines at the C5′ position of the indole compromised cell permeability.[17] Evaluation of the piperidine derivative 19 revealed not only that cell potency could be dramatically improved[18] by removal of one of these basic amines, but that the primary amine in 17 was not contributing to intrinsic potency. With the discovery of the cell potency-enhancing C5′ piperidine, a more detailed exploration of the quinolinone C6 SAR was conducted.

A set of 6-substituted-5′-piperidinyl-indolyquinolinones was prepared (Table 2). With a bromide handle, Suzuki
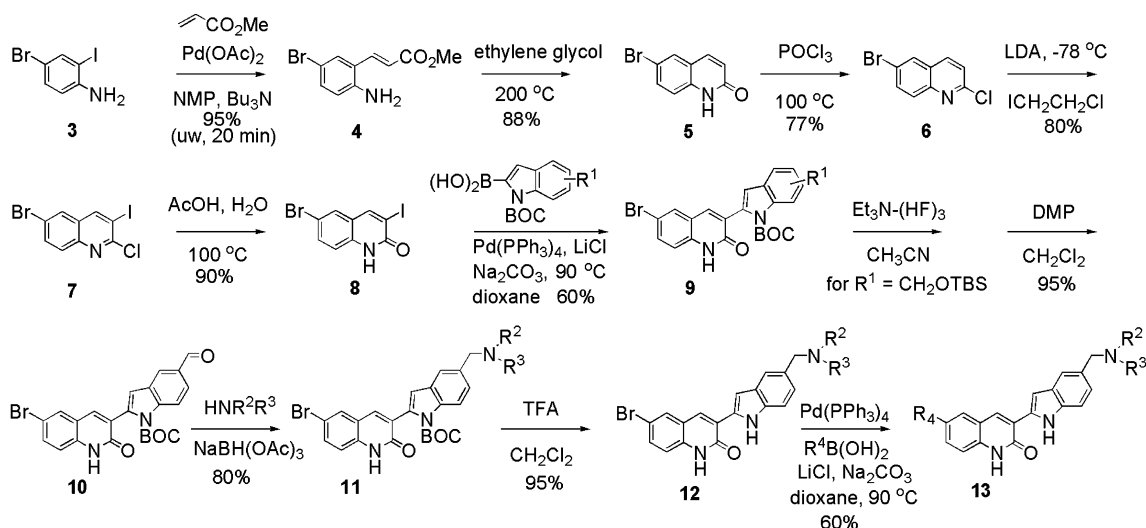
Scheme 1. Synthesis of 6-substituted indolylquinolinones.

Table 1. Inhibition data for indolylquinolinone analogs

Compound	Structure	Chek1[a] IC$_{50}$ (nM)	Cell EC$_{50}$ (nM)
14		1000	
2		140	
15		580	
16		190	
17		4.0	3700
18		0.70	3900
19		4.6	170

[a] Tested at 0.1 mM ATP.

coupling and copper-mediated Ullmann coupling reactions[19] were used to survey potential groups. Amides and 5-membered ring heterocycles such as **21–28** provided Chek1 inhibitors with excellent potency against the enzyme, although some compounds (**21**, **27**) again appeared to have compromised cell potency. Of particular interest was the pyrazole-containing inhibitor **22** which best balanced intrinsic and cell-based potency. A few phenols were also incorporated[8,9] (**30** and **31**), yet these resulted in compounds with diminished potency. The general observation was made that potent inhibitors with high PSA (>100 Å^2)[20] yielded poor cell potency, as in **21** and **27**, possibly due to impaired cell permeability. PSA has been previously correlated to cell permeability[21] and other drug transport properties.[22] Experimental log P values for this series do not correlate well with the loss in cell potency and were within a 'drug-like' range (i.e., log P for **22** = 2.81).
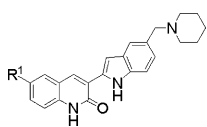
An analysis of the binding mode of **22** allowed us to hypothesize as to the unexpected potency of polar substituents oriented toward the hydrophobic region I. Given that X-ray crystallographic structures cannot resolve hydrogen atoms, we postulate that the pyrazole in **22** hydrogen bonds to water in hydrophobic region I and helps to stabilize these moieties in the binding pocket. As can be seen in Figure 3,[5] the pyrazole group of **22** can hydrogen bond to either of the front two water molecules, one of the acidic oxygens of Asp148, and the basic nitrogen of Lys38 (not shown) *in addition to* the backbone interactions made by this class of inhibitors (see Figure 2). Furthermore, an analysis of the limited SAR presented in Table 2 suggests the importance of correctly coordinating these water molecules with
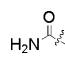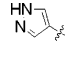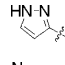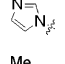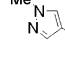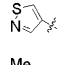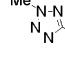
H-bond acceptors (e.g., **21**, **22**, **25**, **26**, and **28**). Removing the outer H-bond acceptor, as in **23**, **24** or **29**, leads to a decrease in potency.

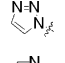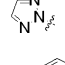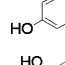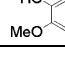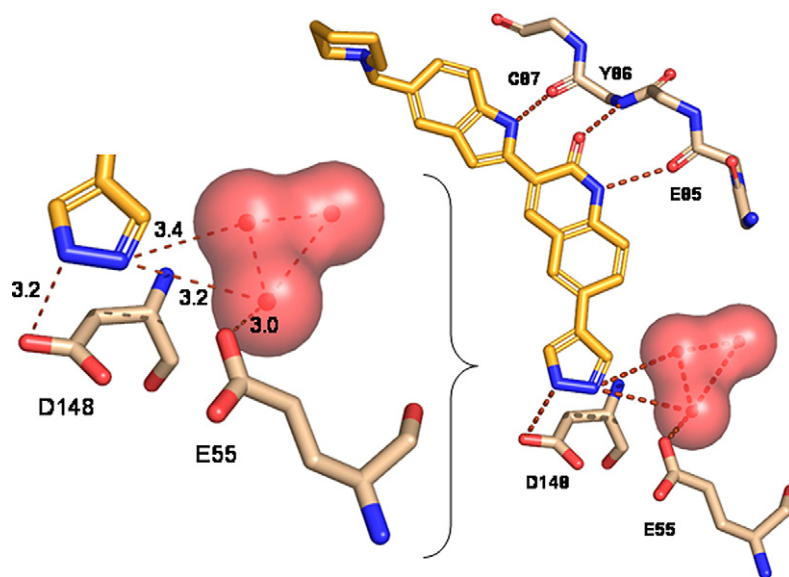Following the selection of pyrazole as a suitable C6 substituent, efforts returned to the C5′ indole position in order to further optimize potency and to begin exploring pharmacokinetics. Earlier efforts in this series[23] indicated that this group was a primary site of oxidative metabolism and that improved PK profiles could be obtained through reducing its oxidative potential. Cell potency/permeability was easily influenced by the character of this substitution, and again the trend was noted that high molecular PSA resulted in poor cell potency (i.e., **34**, **35**). The strategy that emerged was to combine potency enhancing groups at C6 and C5′ that minimized PSA.
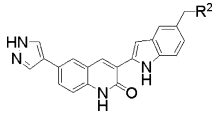
Finally, the pharmacokinetic profile of these compounds was studied in dog (Table 3). Plasma clearance for compounds **22**, **32–35** was moderate with half-lives ranging from 1.5 to 4.4 h. Clearance was improved with **36** by capping the pyrazole with a methyl group albeit with reduced potency. Considering cellular potency as well as PK profile, compounds **22** and **32** emerged out as lead compounds in this indolylquinolinone series.
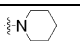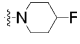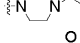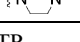
In summary, a series of potent Chek1 inhibitors were discovered based on comparison of the X-ray structure of ATP-competitive HTS leads **1** and **2** bound to Chek1. An efficient synthetic route has been developed to facilitate the SAR studies. A general trend was observed that compounds with multiple basic amines,

Table 2. Inhibition data for C6-substituted indolylquinolinone analogs

Compound	R[1]	Chek1 IC$_{50}$[a] (nM)	Cell EC$_{50}$ (nM)	PSA (Å^2)
20	Br	2.9	460	54
21	H$_2$N(C=O)	0.34	520	102
22	HN–N pyrazole	0.65	97	89
23	HN–N pyrazole	5.6	250	83
24[19]	N=N imidazole	4.3	320	75
25	Me-N pyrazole	1.1	130	74
26	S–N thiazole	0.64	190	69
27[19]	Me-N–N triazole	6.4	1300	103
28[19]	N–N triazole	0.74	230	89
29[19]	N–N–N triazole	14	880	88
30	HO-phenyl	29	6300	79
31	HO/MeO-phenyl	20	>10,000	89

[a] Tested at 0.1 mM ATP.

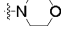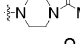**Figure 3.** X-ray crystallographic structure of **22** (yellow) bound to Chek1 (tan). Hydrogen bonds between the inhibitor and Chek1 are shown in dashed lines (maroon). Three conserved water molecules found in H1 are shown as red spheres with their hydrogen bonding network (dashed red lines). Image on left is a detail of the pyrazole hydrogen-bonding environment.

Table 3. Pharmacokinetic profiles of indolylquinolinones

Compound[c]	R[2]	Chek1 IC$_{50}$[a] (nM)	Cell EC$_{50}$ (nM)	PSA (Å^2)	dog PK	
					CL (mL/min/kg)	t$_{1/2}$ (h)
22		0.65	97	89	30	4.4
32		1.0	120	89	22	2.5
33		0.83	170	102	34	2.0
34		2.5	870	111	27	1.5
35		2.1	1142	123	23	2.0
36[b]		3.0	420	98	6.5	4.1

[a] Tested at 0.1 mM ATP.
[b] Pyrazole is *N*-methylated in **36**.
[c] Compounds dosed at 0.25 mpk iv (DMSO) in cassette format.

or high PSA, exhibited diminished cell potency. Minimization of these parameters, resulted in Chek1 inhibitors with improved cell potency. Among these potent Chek1 inhibitors, compounds **22** and **32** were found to be leading compounds with moderate clearance in dogs following intravenous dosing.

References and notes

1. (a) Zhou, B. B.; Bartek, J. *Nat. Rev. Cancer* **2004**, *4*, 1; (b) Bartek, J.; Lukas, J. *Cancer Cell* **2003**, *3*, 421.
2. Kong, N.; Fotouhi, N.; Wovkulioch, P. M.; Roberts, J. *Drugs Future* **2003**, *28*, 881.
3. Kawabe, T. *Mol. Cancer Ther.* **2004**, *3*, 513.
4. Prudhomme, M. *Recent Patents Anti-Cancer Drug Discov.* **2006**, *1*, 55.
5. Compounds **1**, **2** or **22** were diffused into pre-formed apo Chek1 crystals. The X-ray diffraction data were collected from these Chek1 inhibitor complex crystals to 1.8, 2.0, and 1.7 Å resolution with R_{sym} = 0.067, 0.093, 0.063 and completeness = 96%, 94%, 98%, respectively. The complex structures were refined to an R-factor of 0.24, 0.23, and 0.23, respectively. The detailed X-ray diffraction data and refinement statistics are listed under PDB code 2HXL, 2HXQ, and 2HY0 at the protein data bank.
6. Fraley, M. E.; Steen, *J. Bioorg. Med. Chem. Lett.* **2006**, in press.
7. Traxler, P.; Furet, P. *Pharmacol. Ther.* **1999**, *82*, 195.
8. Foloppe, N.; Fisher, L. M.; Francis, G.; Howes, R.; Kierstan, P.; Potter, A. *Bioorg. Med. Chem.* **2006**, *14*, 1792.
9. Lin, N.-H.; Xia, P.; Kovar, P.; Park, C.; Chen, Z.; Zhang, H.; Rosenberg, S. H.; Sham, H. L. *Bioorg. Med. Chem. Lett.* **2006**, *16*, 421.
10. Ni, Z.-J.; Barsanti, P.; Brammeier, N.; Diebes, A.; Poon, D. J.; Ng, S.; Pecchi, S.; Pfister, K.; Renhowe, P. A.; Ramurthy, S.; Wagman, A. S.; Bussiere, D. E.; Le, V.; Zhou, Y.; Jansen, J. M.; Ma, S.; Gesner, T. G. *Bioorg. Med. Chem. Lett.* **2006**, *16*, 3121.
11. All compounds were characterized by ^{1}H NMR and high resolution mass spectrometry. Experimental procedures will be published in a submitted patent by these authors.
12. Kondo, Y.; Inamoto, K.; Sakamoto, T. *J. Comb. Chem.* **2000**, *2*, 232.
13. Marsais, F.; Godard, A.; Queguiner, G. *J. Heterocyclic Chem.* **1989**, *26*, 1589.
14. Fraley, M. E.; Arrington, K. L.; Buser, C. A.; Ciecko, P. A.; Coll, K. E.; Fernandes, C.; Hartman, G. D.; Hoffman, W. F.; Lynch, J. J.; McFall, R. C.; Rickert, K.; Singh, R.; Smith, S.; Thomas, K. A.; Wong, B. K. *Bioorg. Med. Chem. Lett.* **2004**, *14*, 351.
15. Chek1 inhibitory activity was measured using a homogeneous time-resolved fluorescence assay which measures phosphorylation of a biotinylated GSK-3 peptide as described in Barnett et al., *Biochem J.* **2005**, *385*, 399. For the construct, a naturally occurring exon 10 splice variant of human Chek1 described in patent application US20050266469(A1), containing primarily the kinase domain, was expressed in baculovirus with a C-terminal 6-histidine tag. This protein was purified on a Ni affinity column and used as it is for kinetic assays, or purified further on Heparin and SEC columns for crystallography. The Chek1 concentration was 0.5 nM and ATP was used at 0.1 mM. IC$_{50}$ values are reported as the averages of at least two independent determinations; standard deviations are within ±25–50% of IC$_{50}$ values.
16. NCI-H1299 lung carcinoma cells were arrested with 16-h treatment of camptothecin, and then treated with Chek1 inhibitors for additional 8 h. Checkpoint escaped mitotic index due to Chek1 inhibition was assessed by measuring the mitotic-specific phosphorylation of nucleolin in Chek1 inhibitor-treated cells using an antibody-coated, bead-based assay. In this assay, total nucleolin is captured on a streptavidin-coated paramagnetic bead coupled with biotinylated nucleolin monoclonal antibody 4E2 (Research Diagnostics, Inc.). Phosphorylated nucleolin is detected by an antibody complex consisting of a phospho-specific nucleolin monoclonal antibody TG3 (Applied NeuroSolutions, Inc.) and a ruthenylated goat anti-mouse IgM antibody labeled with ruthenylation kit (BioVeris Corp).

The electrochemiluminescent complex is quantified with BioVeris M-8 Analyzer. The EC_{50} of checkpoint escape mediated by Chek1 inhibition was determined with 10-point series diluted Chek1 inhibitor-treated tetraplicate cell samples.

17. Chek1 inhibitors in another report also showed diminished cell potency and the authors also suspect cell permeability: Li, G.; Hasvold, L. A.; Tao, Z.-F.; Wang, G. T.; Gwaltney, S. L., II; Patel, J.; Kovar, P.; Credo, R. B.; Chen, Z.; Zhang, H.; Park, C.; Sham, H. L.; Sowin, T.; Rosenberg, S. H.; Lin, N.-H. *Bioorg. Med. Chem. Lett.* **2006**, *16*, 2293.

18. Note that Chek1 inhibitory activity is measured at K_m for ATP (0.1 mM). In the cell assay, the ATP concentration is 2.0 mM resulting in an inherent 10-fold potency shift between these assays.

19. For preparation of triazole, **28**, **29** and tetrazole, **27**, see: (a) Wu, Y-J.; He, H.; L'Heureuk, A. *Tetrahedron Lett.* **2003**, *44*, 4217; (b) Ullmann, F. *Ber. Dtsch. Chem. Ges.* **1903**, *36*, 2382, For review; (c) Lindley, J. *Tetrahedron* **1984**, *40*, 1433.

20. PSA calculations are done using the method published by Clark. Clark, D. E. *J. Pharm. Sci.* **1999**, *88*, 807.

21. Papageorgiou, C.; Gamenish, G.; Borer, X. *Bioorg. Med. Chem. Lett.* **2001**, *11*, 1549.

22. Ertl, P.; Rohde, B.; Selzer, P. *J. Med. Chem.* **2000**, *43*, 3714.

23. Fraley, M. E.; Hoffman, W. F.; Arrington, K. L.; Hungate, R. W.; Hartman, G. D.; McFall, R. C.; Coll, K. E.; Rickert, K.; Thomas, K. A.; McGaughey, G. B. *Curr. Med. Chem.* **2004**, *11*, 709.